



ISSN: 1813-162X (Print); 2312-7589 (Online)
Tikrit Journal of Engineering Sciences
available online at: <http://www.tj-es.com>

TJES
Tikrit Journal of
Engineering Sciences

Flow simulation over semicircular labyrinth weir using ANSYS -fluent

[Jehan M. Fattah Sheikh Suleimany¹ *](#), [Tara H. Aurahman²](#), [Bruska S.Mamand³](#)

Department of Water Resource Engineering/College of Engineering/Salahaddin University/ Erbil/ Kurdistan Region/Iraq.

Keywords:

Semi- circular weirs, discharge coefficient, ANSYS, k-epsilon turbulence.

ARTICLE INFO

Article history:

Received 30 Sep. 2021
Accepted 01 Apr. 2022
Available online 22 Apr. 2022

©2021 COLLEGE OF ENGINEERING, TIKRIT UNIVERSITY. THIS IS AN OPEN ACCESS ARTICLE UNDER THE CC BY LICENSE
<http://creativecommons.org/licenses/by/4.0/>



Citation: Sheikh Suleimany JMF, Aurahman TH, Mamand BS. Metallic Oxides for Innovative Refrigerant Thermo-Physical Properties: Mathematical Models. Tikrit Journal of Engineering Sciences 2022; 29(1): 59-74.
<http://doi.org/10.25130/tjes.29.1.6>

A B S T R A C T

This study investigates the flow of a semicircular labyrinth weir in an open channel by experimental and numerical methods. The experiments were carried out in a channel with a length of 3.5m and width of 0.25m and 0.3m height under five different flow rates. Five different discharge values over the weir were used. In each experiment, flow rate and flow depth were measured. Numerical processes solved using mathematical equations of fluid flow through the computational fluid dynamics using ANSYS FLUENT code. The Volume of Fluid (VOF) model is designed for the case of water and air-immiscible faces. Standard k-epsilon turbulence models were tested. A mass balance result indicates that the maximum error between the inlet and outlet discharges of the main channel does not exceed 12% for discharge values of 4.31 L/sec. The results indicate that by increasing the discharge flow rate, the percentage of error decreased to 0.4% for discharge, 14.6 L/sec. The findings show that the free water surface profile obtained from the numerical model compared to experimental values complies well with the experimental results.

* Corresponding Author: %20jehanmohammed.sheikhsuleimany@su.edu.krd, Department of Water Resource Engineering/College of Engineering/Salahaddin University/ Erbil/ Kurdistan Region/Iraq.

محاكاة التدفق فوق هدار المتاهة النصف دائري باستخدام ANSYS –fluent

الخلاصة

تبحث هذه الدراسة في التدفق على الهدارة نصف دائري القناة المفتوحة تجريبياً وعددياً. أجريت التجارب في قناة بطول 3.5 م وعرض 0.25 م وارتفاع 0.3 م تحت خمسة معدلات تدفق مختلفة. تم استخدام خمس قيم تصريف مختلفة على السد. في كل تجربة ، تم قياس معدل التدفق وعمق التدفق تم حل العمليات العددية باستخدام المعادلات الرياضية لتدفق السوائل من خلال ديناميات السوائل الحسابية باستخدام كود ANSYS FLUENT القياسي. تم تصميم موديل حجم السوائل (VOF) لحالة الوجوه المائية غير القابلة للامتزاج بالماء والهواء. تم اختبار نماذج الاضطراب القياسية k-epsilon. تشير نتيجة توازن الكتلة إلى أن الحد الأقصى للخطأ بين تصريفات المدخل والمخرج للقناة الرئيسية لا يتجاوز 12 % لقيم التصريف البالغة 4.31 لتر/ثانية. تشير النتائج إلى أنه من خلال زيادة معدل تدفق التصريف ، انخفضت نسبة الخطأ إلى 0.4 % للتصريف 14.6 لتر/ثانية. تظهر النتائج أن أن السطح المائي الحر الذي تم الحصول عليه من النموذج العددي مقارنة بالقيم التجريبية يتوافق بشكل جيد مع النتائج التجريبية.

1. INTRODUCTION

A labyrinth weir is a specific type of nonlinear weir with a different shape in the plan view. The walls of labyrinth weirs are connected in plan in the form of trapezoidal, semicircular, triangle, rectangular and curved shapes. These types of weirs have a longer crest and higher discharge passes through them under load or equivalent height. They also have better performance in low hydraulic loads; however, their hydraulic efficiency is gradually decreased as a result of increasing load, leading to the decrease of their water transmissivity[2]. Labyrinth weirs are generally considered economic structures, labyrinth weirs are used in regions that have limitations in terms of place and total width increase of weir location and/or have had limitations for flood in terms of space capacity and additional volume increase well as for modifying and increasing existing weir capacity. [16]

In the present study, a physical model of a semicircular weir was investigated experimentally in the lab and numerically by using ANSYS -fluent code. The discharge capacity of water flowing above the weir and its flow profile tested for the k-epsilon turbulence model. Many researchers studied flow over weirs using numerical simulations as follows: Korkmaz and Ghaznawi [8] conducted a numerical simulation of the flow over a broad-crested weir based on the standard k-epsilon turbulence closure model. The computed free-surface profiles based on the volume-of-fluid (VOF) method were in good agreement with the measured results. Carrillo et. al. [1] conducted numerical simulations of subcritical flow downstream of a labyrinth weir using the ANSYS CFX. Their results were compared with experimental data previously acquired on a fairly large-scale flume, including a trapezoidal labyrinth weir with a quarter-round crest profile and sidewall angle α equal to 30° . They showed that fairly good agreement was obtained on the main flow properties downstream of the weir, such as flow depths, bottom pressure heads, and velocities sufficiently distant from the invert, except in the vicinity of the weir.

Khalili and Honar [9] carried out a comprehensive laboratory study on a physical model of a semi-circular labyrinth side weir and the model was evaluated for three heights and three radii. They investigated the hydraulic effects of the side weir on increasing discharge capacity. They found that the dimensionless parameters of weir height, weir length, nape height, and upstream Froude number affected discharge coefficient (C_d). Yuce et. al. [16] presented a computational fluid dynamics (CFD) simulation to investigate the effects of the obliqueness of cylindrical weirs on the flow velocity distribution, the pressure distribution, and the distribution of water depth over the weir crest. Their results show that flow patterns are affected by the inclination angle with respect to the flow direction. They noticed that the inclination angle increment increases the velocity of flow at the downstream surface of the weir, and thus increases the absolute value of the negative pressure, at the inward-moved end of the weir. Jiang et.al. [12] analyzed the effect of the upstream angle on flow over a trapezoidal broad-crested weir based on numerical simulations using toolbox Open FOAM trapezoidal broad-crested weir configurations with different upstream were studied under free-flow conditions. The volume-of-fluid (VOF) method and two turbulence models (the standard k- ϵ model and the SSTk- ω model) were presented in numerical simulations. Shaghaghian and Sharifi[5] attempted to investigate the characteristics of flow in triangular labyrinth weirs through FLUENT Software. In this regard, using GAMBIT Model, geometrical and grid generation conditions of flow were created for flow field solution. Using numerical models of Fluent, boundary conditions and flow field conditions were implemented for the models. Safarrazavi Zadeh et. al. [14] experimentally investigated the flow over labyrinth weirs with semicircular and sinusoidal shapes in rectangular flumes using a different rate of discharge capacity. The equation for predicting the discharge coefficient of labyrinth weirs for both types was presented. Noori [11] improved the discharge

capacity of oblique weirs experimentally by rounding the weir crests and testing the values of coefficient of discharge (C_d) for different weir heights, oblique angle, and crest diameter. He showed that circular crested oblique weirs offered higher discharge capacity compared with some other weir shapes. He found that values of discharge coefficient (C_d) decreased slightly with the increase of the head of water over the weir and increased with an increase in weir height and diameter of the crest and weirs of small oblique angles gave lower values of (C_d). Ehsanifar and Ghodsian [4] studied a piano key weir with an upstream nose and semicircular crest at the outlet experimentally and numerically, they found that the discharge coefficient (C_d) increased by about 14%. The significance of this study came from that the previous studies focused on different types of labyrinth weir, but less attention was given to the labyrinth weir with a semi-circular shape because the flow over these types of weirs is three-dimensional,

and is complicated to compute the surface profile experimentally. The goal of this study is to perform numerical simulations to examine the hydraulic performance of semi-circular labyrinth weir in terms of free-surface profile, velocity streamlines, isosurface, water volume fraction, pressure distribution, and flow separation zone. In addition, the free surface profiles computed from the experimental study were compared to the numerical calculation using ANSYS-fluent

2. THEORETICAL BACKGROUND

2.1 Discharge Equation:

Applying the continuity equation to a section on the semicircular labyrinth weir as shown in Fig.1 weir crest where the flow is at critical depth, and the weir developed crest length (L) with the rectangular cross-sectional area of the channel with (w), the discharge (Q) was as shown in Eq. (1). [13].

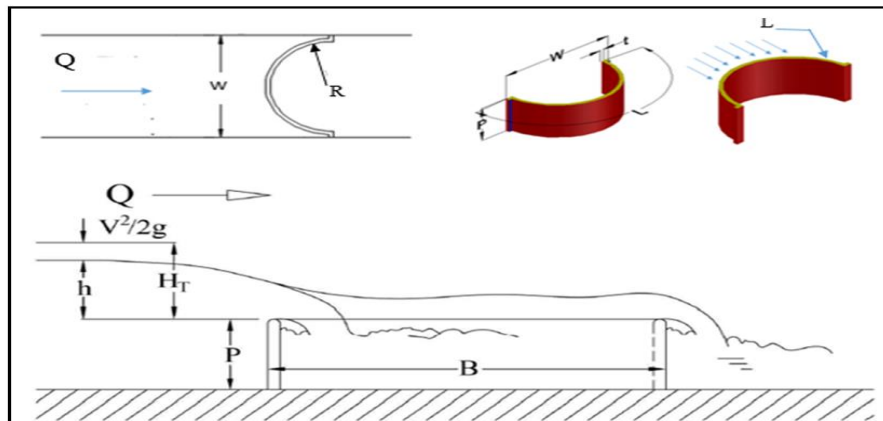


Fig.1. Definition sketch of flow over semicircular weir.

$$Q = \frac{2}{3} C_d \sqrt{2g} L H_T^{1.5} \dots\dots\dots 1$$

Where:

Q : discharge passing through the weir in L/sec

C_d : Coefficient of the discharge unit less

L : Developed crest length of semicircular weir (m)

H_T : Total head of water over the weir ($H_T = h + \frac{v^2}{2g}$) (m)

h : Head of water over the weir in meters

g : Acceleration due to gravity m^2/s

w :Width of channel (m)

t : Thickness of semi-circular wall (m)

$\frac{v^2}{2g}$: Kinetic head in (m)

p :Height of weir (m)

B : Side wall length of weir (m)

y_1 : Depth of water in the channel (m)

R : Radius of semicircular shape (m)

2.2 Numerical Model Set-up

Numerical codes based on the finite volume method were solving the complex partial differential equations of fluid flow passing over the weir. This will be done through the computational fluid dynamics (CFD). In order to obtain a wide range of flow characteristics with semi-circular weirs, experimental data in the literature was studied numerically by FLUENT code interfaced on ANSYS

V.14. [5,6] The governing equation for fluid motion was named as Navier-Stokes. These equations are non-linear differential equations; therefore, they admit a number of analytical solutions. Navier-Stokes equation consists of a continuity equation in which it's three dimensional forms for unsteady viscous fluid is presented by Desai and Patil [3] as follows:

$$\begin{aligned} \frac{\partial u}{\partial t} + \frac{1}{V_F} \left(u A_x \frac{\partial u}{\partial x} + v A_y \frac{\partial u}{\partial y} + w A_z \frac{\partial u}{\partial z} \right) \\ = - \frac{1}{\rho} \frac{\partial p}{\partial x} + G_x \\ + f_x \dots \dots \dots 2 \\ \frac{\partial v}{\partial t} + \frac{1}{V_F} \left(u A_x \frac{\partial v}{\partial x} + v A_y \frac{\partial v}{\partial y} + w A_z \frac{\partial v}{\partial z} \right) \\ = - \frac{1}{\rho} \frac{\partial p}{\partial y} + G_y \\ + f_y \dots \dots \dots 3 \\ \frac{\partial w}{\partial t} + \frac{1}{V_F} \left(u A_x \frac{\partial w}{\partial x} + v A_y \frac{\partial w}{\partial y} + w A_z \frac{\partial w}{\partial z} \right) \\ = - \frac{1}{\rho} \frac{\partial p}{\partial z} + G_z \\ + f_z \dots \dots \dots 4 \end{aligned}$$

Where

Ax,Ay,Az: Fractional areas open to flow in direction (x,y,z).

u,v,w: Velocities in (x, y, z) direction respectively.

fx,fy,fz: Viscous accelerations in (x, y, z) direction respectively.

Gx,Gy,Gz: Body accelerations

VF: Fractional volume opens to flow.

It is supplemented by the mass conservation equation:

$$\frac{\partial u}{\partial x} A_x + \frac{\partial v}{\partial y} A_y + \frac{\partial w}{\partial z} A_z = 0 \dots \dots \dots 5$$

Volume of fluid (VOF) method is surface tracking technique. This model designed for the case of two or more immiscible fluids (i.e. Able to mix) where the position of the interphase between fluids are of interest (ANSYS FLUENT help) the VOF model was used for tracking liquid-gas (water and air) interphase. FLUENT provided several turbulence models that can solve the multiphase systems with a different number of transport equations. In this study standard k-ε model was used based on the following equations: Desai and Patil [3]

$$\begin{aligned} \frac{\partial(\rho k)}{\partial t} + \frac{\partial(\rho k u_i)}{\partial x_i} = \frac{\partial}{\partial x_j} \left[\left(\mu + \frac{\mu_t}{\sigma_k} \right) \frac{\partial k}{\partial x_j} \right] + G_k + G_b - \rho \varepsilon \\ - Y_M \dots \dots \dots 6 \end{aligned}$$

$$\begin{aligned} \frac{\partial(\rho \varepsilon)}{\partial t} + \frac{\partial(\rho \varepsilon u_i)}{\partial x_i} = \frac{\partial}{\partial x_i} \left[\left(\mu + \frac{\mu_t}{\sigma_\varepsilon} \right) \frac{\partial \varepsilon}{\partial x_j} \right] \\ + C_{1\varepsilon} \frac{\varepsilon}{k} (G_k + C_{3\varepsilon} G_b) \\ - C_{2\varepsilon} \rho \frac{\varepsilon^2}{k} \dots \dots \dots 7 \end{aligned}$$

Gk: Generation of turbulence kinetic energy due to the mean velocity gradients.

Gb: Generation of turbulence kinetic energy due to buoyancy.

YM: Contribution of the fluctuating dilatation in compressible turbulence to the overall dissipation rate.

ρ: Mass density of water. $\frac{kg}{m^3}$

σk,σε: Turbulent Prandtl numbers for k and ε, respectively in standard model

k: Turbulence kinetic energy (m²/sec²)

ε: Turbulence dissipation rate.(m²/sec³)

μt: Turbulent kinetic eddy viscosity (kg/m.sec²)

Constants of Standard k-ε models are:

$$\begin{aligned} C_{1\varepsilon} = 1.44 \quad C_{2\varepsilon} = 1.92 \quad C_\mu = 0.09 \\ \sigma_k = 1 \quad \sigma_\varepsilon = 1.3 \end{aligned}$$

The standard k- ε model

The standard k- ε is a semi –empirical model based on model transport equations for the turbulence kinetic energy and its dissipation rate ε.in the derivation of the k- ε model it was assumed that the flow is fully turbulent. The standard k- ε model is therefore valid only for fully turbulent flows. [12]

The kinetic eddy viscosity is completed by combining k and ε as follows:

$$\mu_t = \rho C_\mu \frac{k^2}{\varepsilon} \dots \dots \dots 8$$

3. METHODOLOGY

3.1 Experimental Work

The experiments were performed on a smooth toughened glass sided and smooth painted bed steel plate channel of 3.5 m working length. The flume cross sectional area is 25 cm wide and 30 cm deep.

Water supplied to the flume from an underground concrete storage tank of internal dimensions (7.5 m length, 2.5 m width and 1.0 m depth). Water drawn from the underground storage tank by an electrically driven centrifugal pump through a 6 inch diameter Steel pipe to the overhead tank providing a total discharge of (50 lit/sec). See Fig.2.

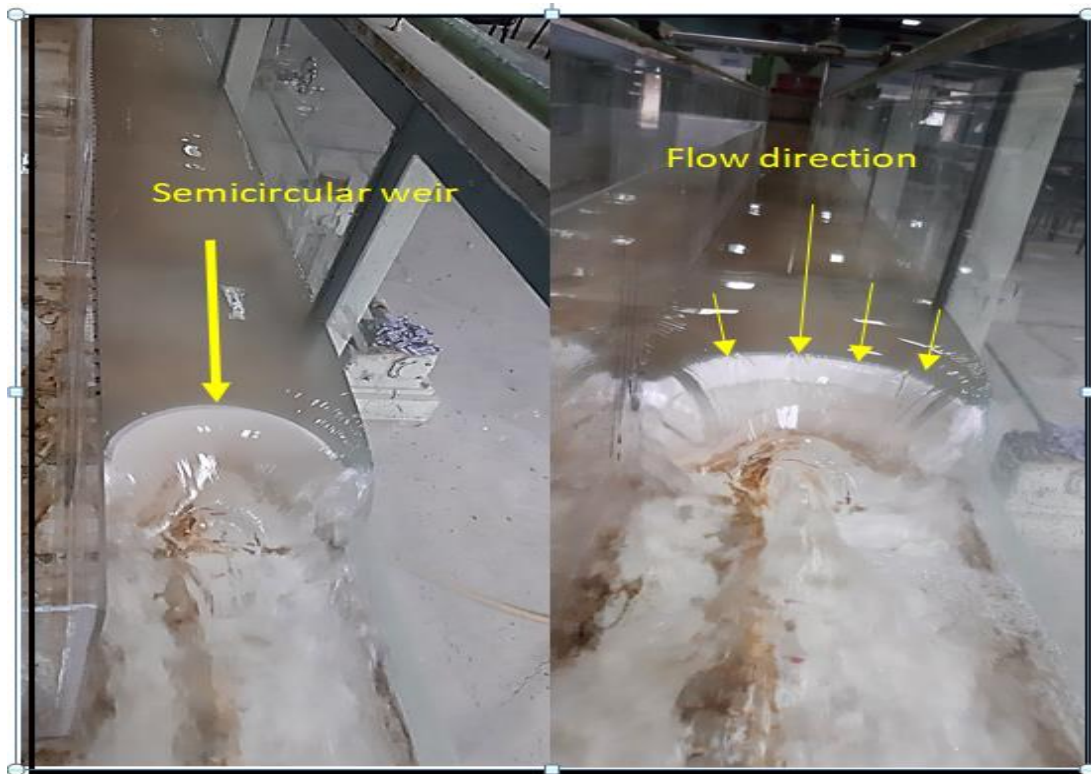


Fig. 2. Schematic diagram of the Open channel with the semicircular weir.

The details of data that taken from an experimental work as indicated earlier were clearly shown in Table 1. For measuring the total discharge passing through the main channel (Q_{in}), a V-notch weir was manufactured at the downstream of the overhead tank. The water depth at upstream of the weir was measured (H_v) and the total channel discharge was calculated using Eq. (9). Mohammed [10]

$$Q_v = 0.0195 H_v^{2.398} \quad \dots \dots \dots (9)$$

Where:

Q_v : discharge over the weir in L/sec, and

H_v : head of the water above the V-notch weir in cm.

To measure the discharge over labyrinth weir, the constructed model of the weir has been installed at 0.4 m from the downstream of the flume. The water depth in the test flume was measured by means of two point gauges. The Vernier scale of the point gages permitted depth readings with an accuracy of 0.05 mm, and the (y_1) is the water depth at the beginning of the flume.

Experimental data of five test runs.

No.	Discharge (L/sec)	y_1 (m)
1	4.31	0.13
2	5.73	0.141
3	9.45	0.157
4	11.3	0.16
5	14.6	0.180

3.2 ANSYS Fluent 14.0

ANSYS CFD is a computational fluid dynamics software tools used by engineers for design and analysis. These tools can simulate fluid flows in virtual environment for example the fluid dynamics of ship hulls; gas turbine engines including the compressors, combustion chamber.

This software follows 5 steps for completion

3.2.1 Model Geometry

Table 1.

Different geometries of semicircular weir were created by using FLUENT code which interfaced on the ANSYS (14.0) software [5,6]. See Fig. 3.

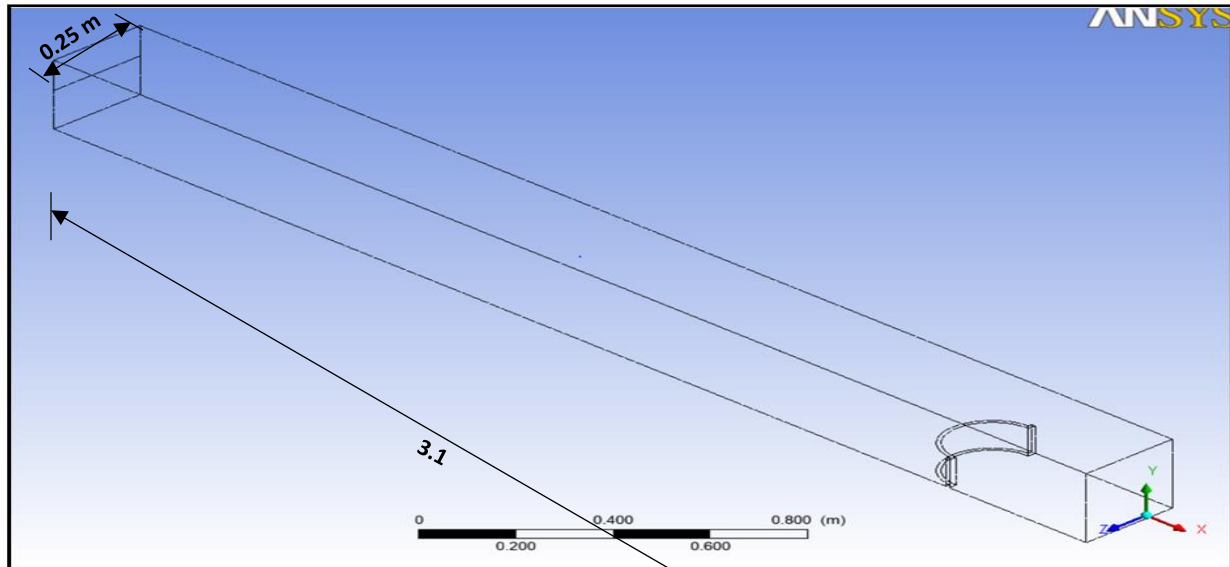


Fig.3. Geometry of an open channel with full width semi-circular weir.

3.2.2 Mesh Geometry

In the present study, the hex dominates mesh method used to calculate mesh grids throughout a solid domain as shown in Fig. 4. Mesh size should be fine enough to ensure the flow features spread out

through all fields. For this purpose, maximum size of grids and maximum face size was examined to be 0.008m as a better mesh density when results compared with existing experimental data. High smoothing option of sizing was turned on and "approximate and curvature" of advanced size function was selected.

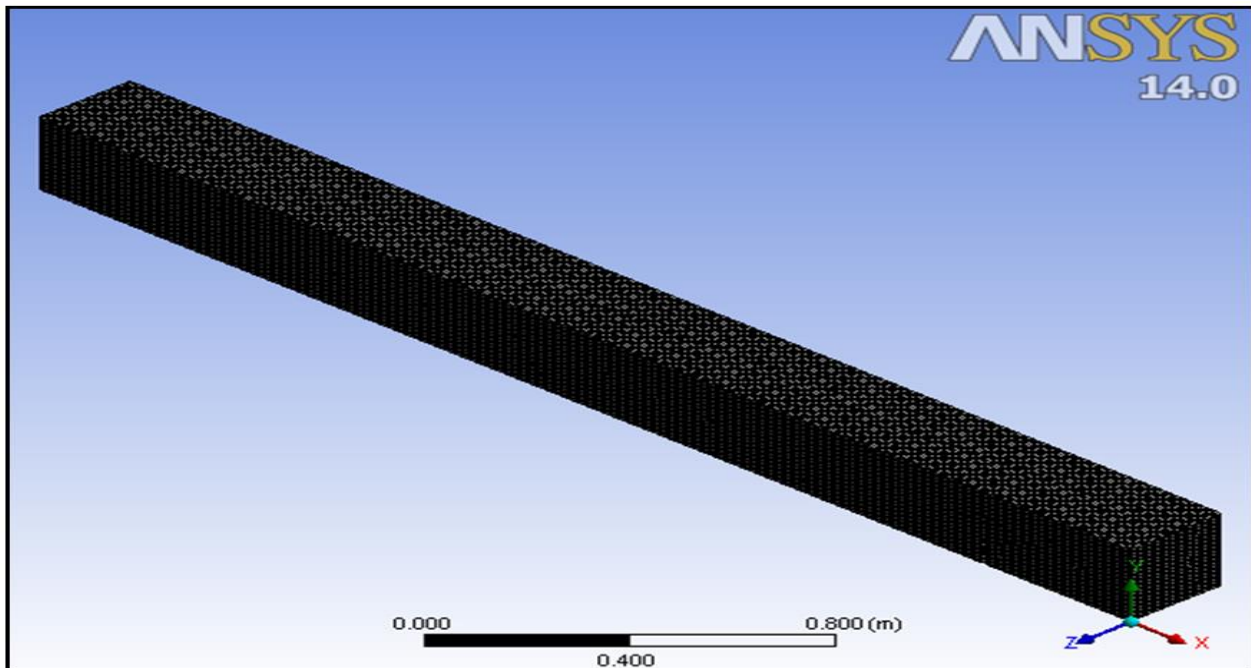


Fig.4. Mesh description of rectangular channel with semi-circular weir .

3.2.4 Boundary and Initial Conditions

The boundary conditions at different positions are explained below and shown in Fig. 5.

- Inlet boundary was defined at the inlet section where water flows only into the channel with a known inlet water depth and the magnitude of inlet velocity that measured from the experiments. It sets to inlet where the air phase entered the domain with zero-gauge total pressure. The fluid values were taken as unit volume fraction in the air and zero for water phase.

- Outlet boundary was defined at the downstream sections where fluid from the domain is exited out. Also, unit return flow volume fraction was putted.
- Top opening of the channel was set as ambient boundary. Zero-gauge pressure and the unit return flow volume fraction in air was required.
- Bottom width, two sides of the channel and weir heights were set as stationary wall that are impermeable to flow, smooth and slipping did not occur.

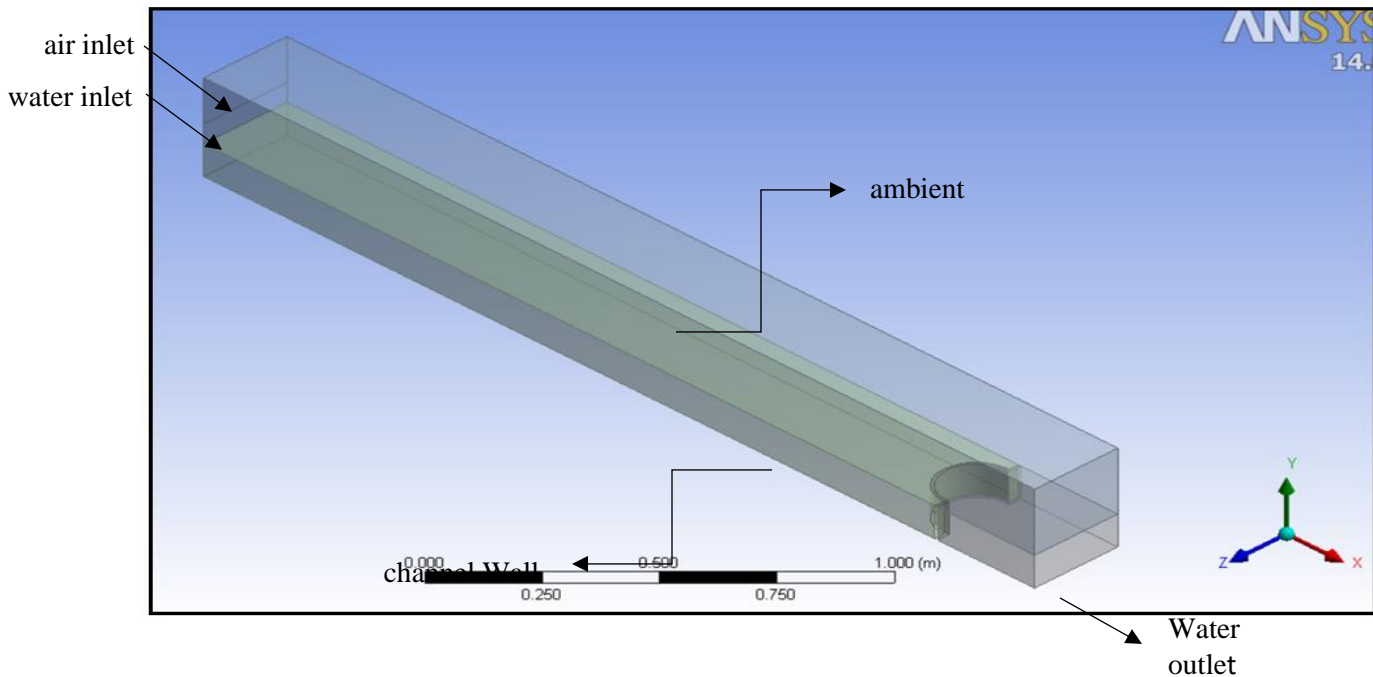


Fig. 5. Locations of boundary conditions.

For the current boundaries, k and epsilon was selected as a specification method for inlet and outlet boundaries, finite volume equations were solved through methods of body force weighted for pressure and second order upwind scheme for mass, momentum and turbulence models. The gravitational acceleration was set as (9.81 m/sec^2) and the operating density of air phase as (1.225 kg/m^3).

3.2.5 Model Runs (Flux report)

Mass imbalance was one of the important criteria for assessing the convergence criteria. The solver flux report showed the differences in mass flow rates at inlet and outlet boundary of the main channel. The balance result will not exactly be zero, but it should

be a small fraction of the net flux through whole domain which displayed in term of (kg/sec).

4. RESULTS AND DISCUSSION

In this study, the water surface profiles along the main channel and above the weir crest were estimated and the results of each part were concluded separately in the following configurations.

4.1 Validation of ANSYS Numerical Program (Mass Balance)

The numerical runs that done by using k-epsilon turbulence model having the following inlet and outlet flow rates inside the flume. The error percent

between inlet and outlet was calculated by the following equation and the results shown in Table 2. In order to check the accuracy of the flow passed over semi-circular weir (Q_{out}), the experimental results of mass balance for seven test runs shown in Table 2. It indicates that the maximum error in the experimental measurements between inlet and outlet discharges of the main channel does not

exceed 12%. This error will occur due to the accuracy of experimental readings by point gauge and the roughness of channel bed. Numerical models calculated flow properties over weir which residual reached to 1×10^{-1} with an accurate mass balance between inlet and outlet discharge as shown in Fig. 6.

Table2.

Experimental and numerical results of the mass balance.

Run	Experimental calculation				Standard k-e		
	H_v (cm)	Q_{in} Eq. (9) (L/sec)	y_1 (cm)	C_d Eq.(1)	Q_{in} (L/sec)	Q_{out} (L/sec)	% Errors Eq.(10)
1	9.5	4.31	0.13	0.79	4	4.55	12
2	11.4	5.73	0.14	0.7	5.76	6.22	7.3
3	13.2	9.45	0.157	0.68	9.442	9.9	4.7
4	14.2	11.3	0.161	0.75	11.29	11.55	2.25
5	15.8	14.6	0.1804	0.63	14.53	14.59	0.4

%Error

$$= \frac{|Q_{out_{numerical}} - Q_{out_{experimental}}|}{Q_{out_{experimental}}}$$

* 100 10

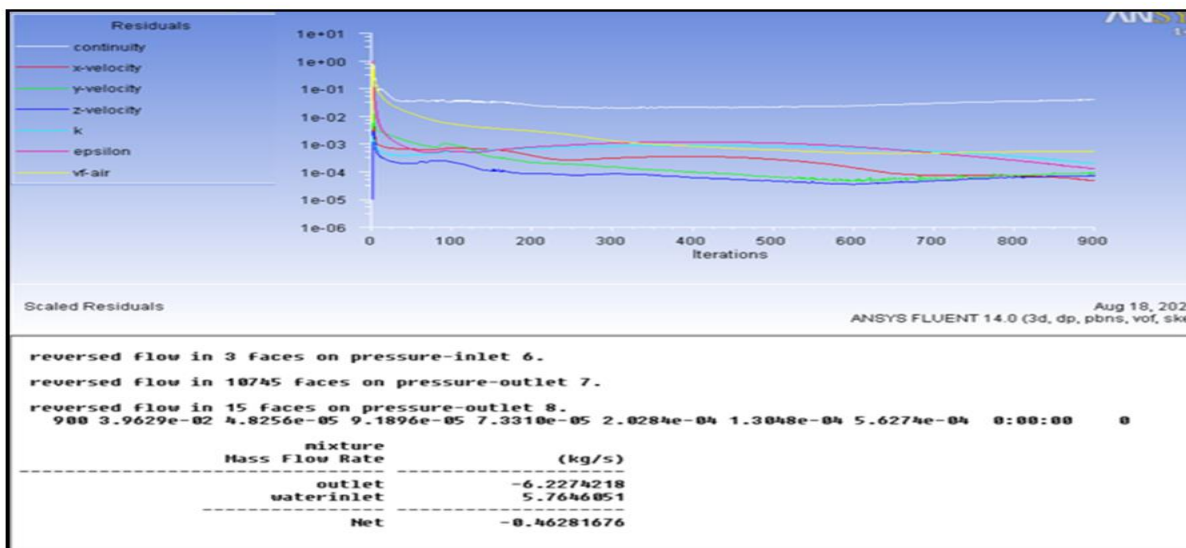


Fig. 6. Residual window and mass balance results

4.2 Water Surface Profiles

This section shows the longitudinal water surface profile for subcritical flow regime inside the flume.

As explained before, the numerical results depend up on the experiments. The free surface profile in the laboratory was shown in Fig. 7.

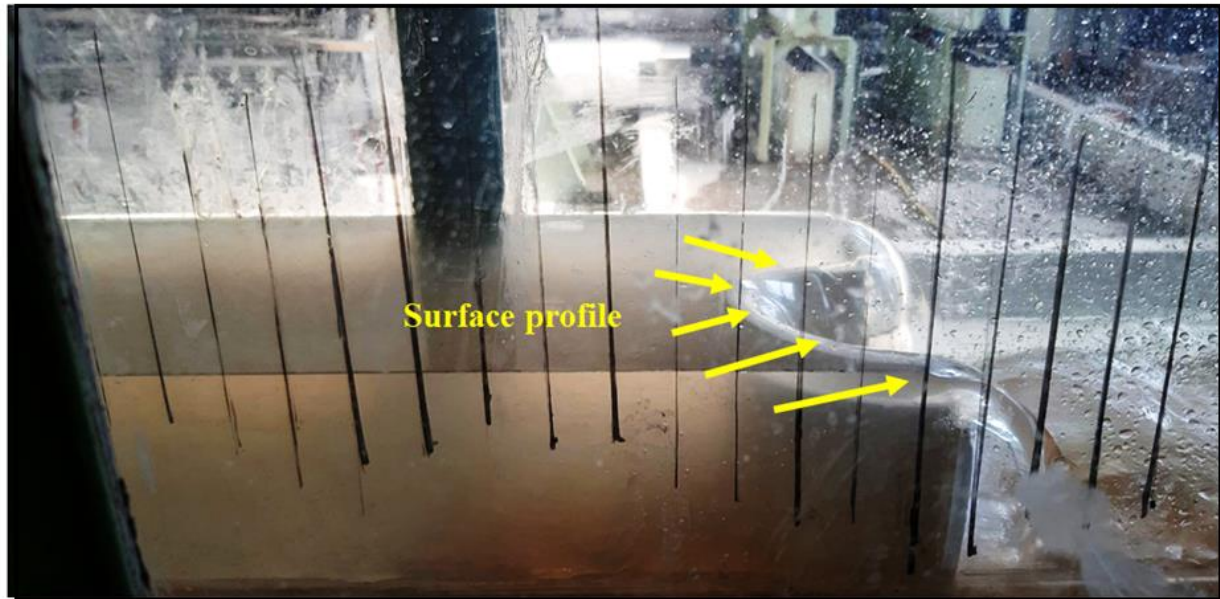


Fig.7. Experimental free surface profile above semicircular weir.

For numerical investigations the contours of water volume fraction were plotted as shown in Fig. 8. The depth measurements were taken at the centreline of

the main channel. In which the contours of water volume fraction were plotted on a rectangular plane and a polyline of water

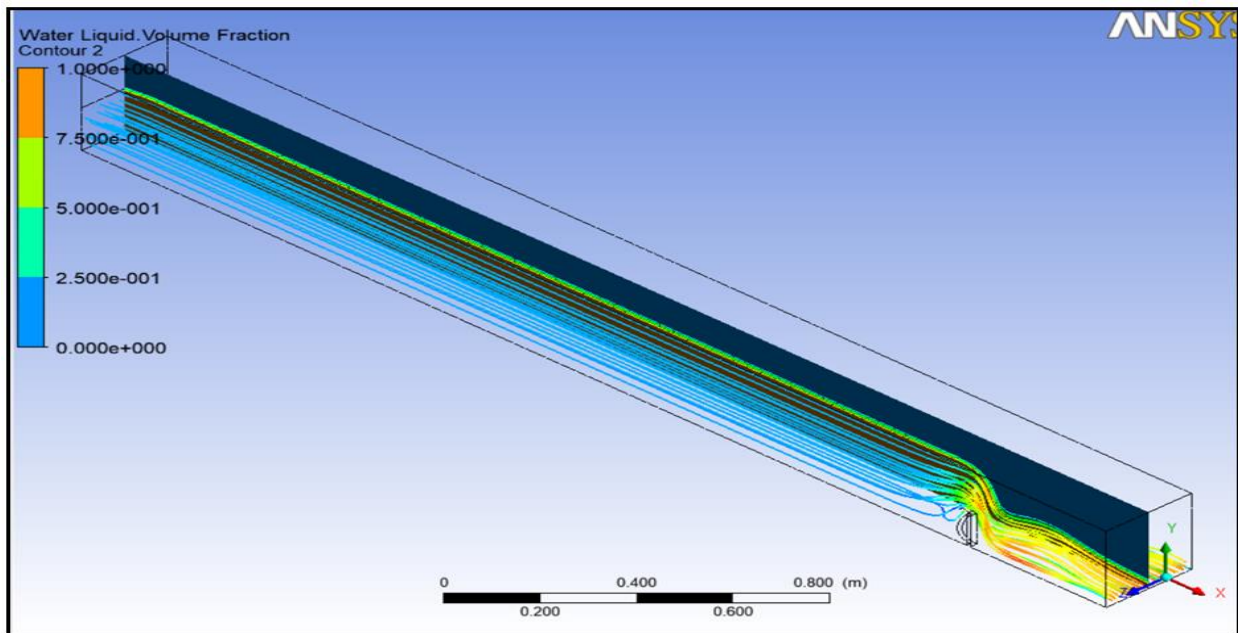


Fig.8. Water depth measurements at the centreline of the channel with semi -circular weir

Five different discharge values over the weir were used. Set of figures was plotted to make a comparison between standard k- ϵ turbulence model and experiments with different run discharges. Figs.

9 – 13 show the x-axis of the graph represents the distance from the inlet channel boundary and y-axis represents the water height from the bottom of the channel.

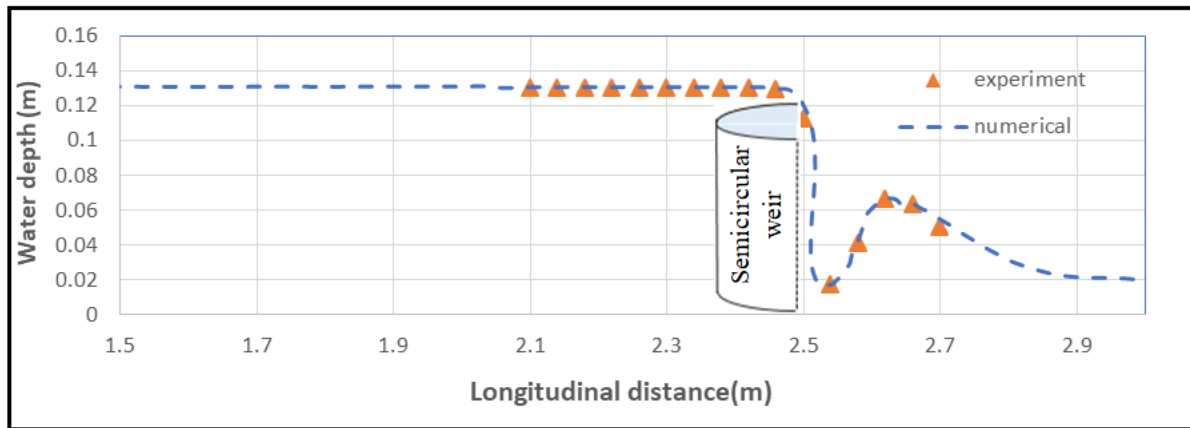


Fig. 9. Comparison of water surface profile by standard k- ϵ and experiment for $Q_{in} = 4.31$ L/sec.

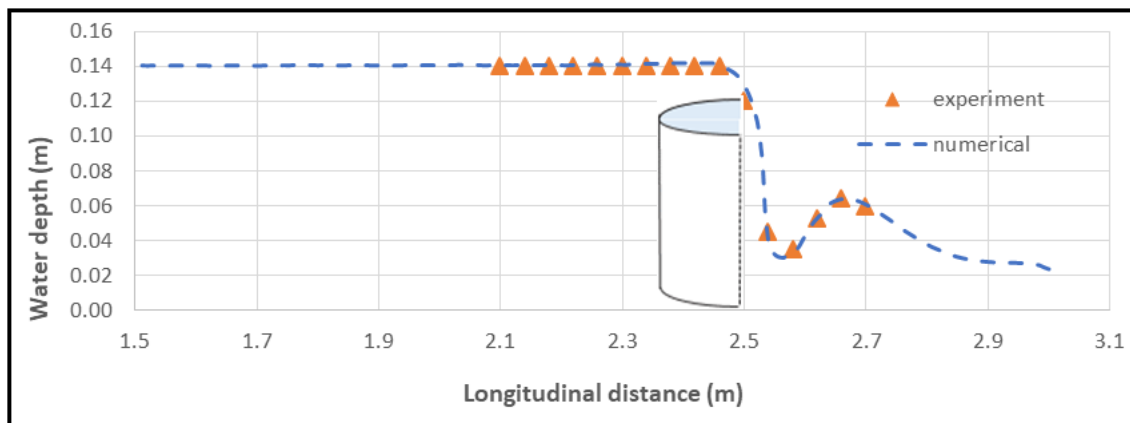


Fig.10. Comparison of water surface profile by standard k- ϵ and experiment for $Q_{in} = 5.73$ L/sec.

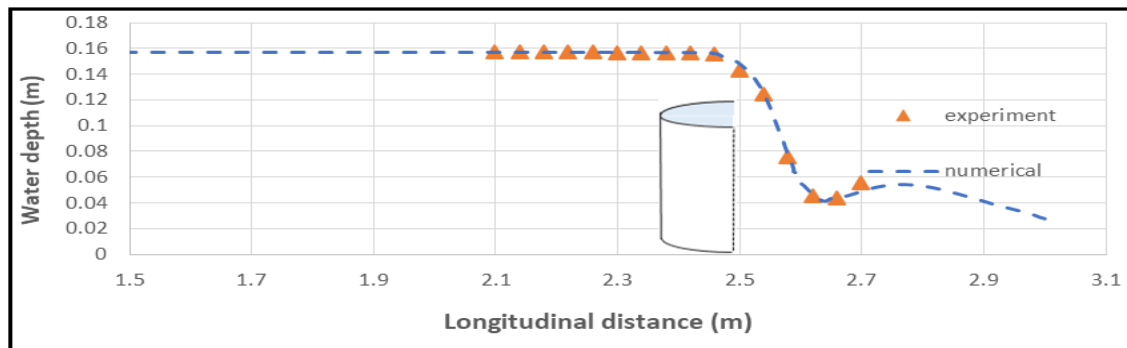


Fig.11. Comparison of water surface profile by standard k- ϵ and Experiment for $Q_{in} = 9.45$ L/sec.

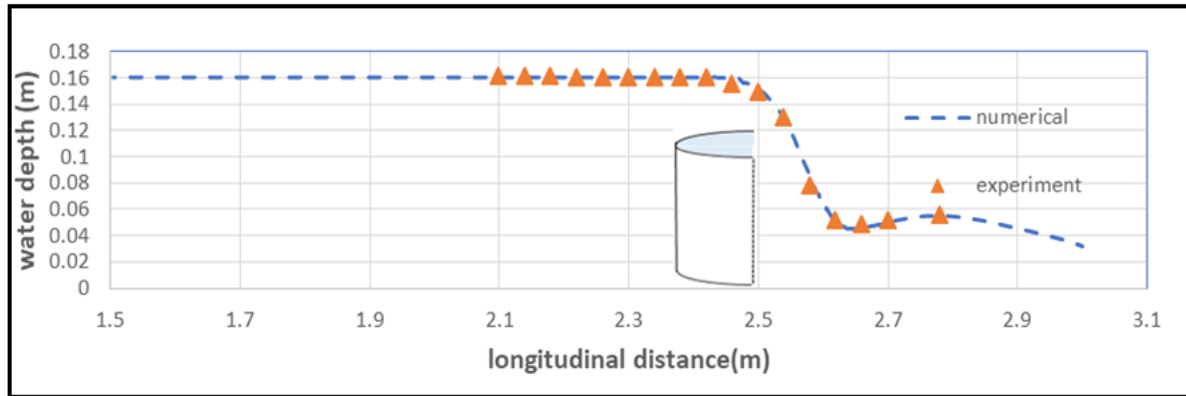


Fig.12. Comparison of water surface profile by standard $k-\epsilon$ and experiment for $Q_{in} = 11.3$ L/sec.

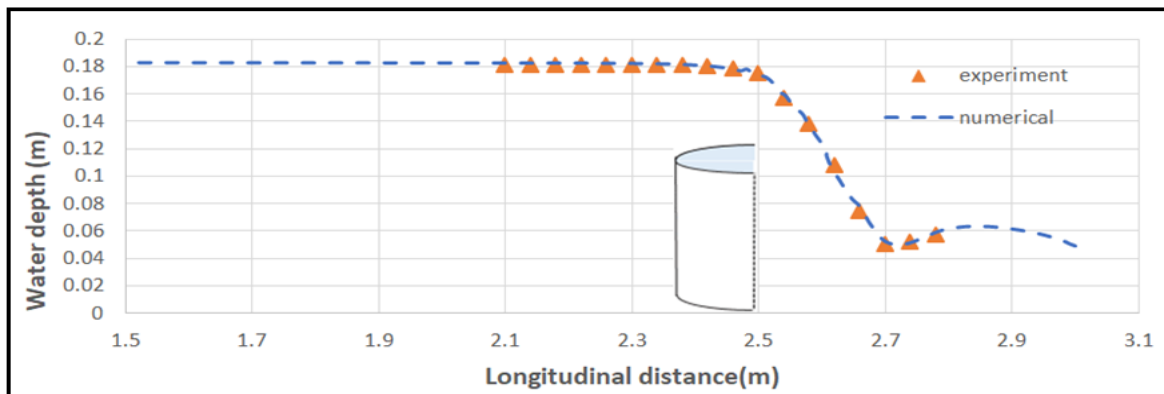


Fig.13. Comparison of water surface profile by standard $k-\epsilon$ and experiment for $Q_{in} = 14.6$ L/sec.

4.3 Velocity Distributions

Seed points of velocity streamlines was generated and then spread out at the water inlet boundary section. These streamlines which moves through the main channel domain was divided into surface,

intermediate and bed lines basing on their position which moves through. Figs.14 - 18 show the streamlines move directly from upstream of the main channel to pass over the semi-circular weir and then dropped by a curve and continues toward the downstream outlet of the main channel.

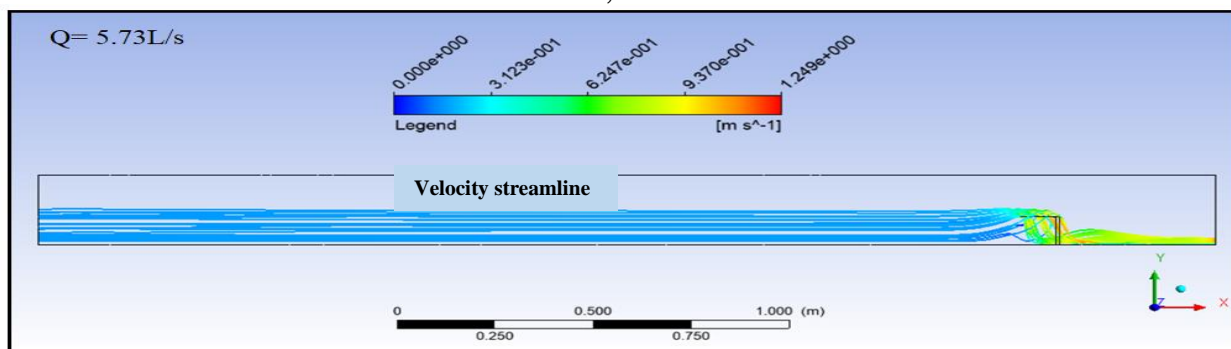


Fig. 14. Streamline layout above weir for $Q = 5.73$ L/sec and $P = 0.1$ m.

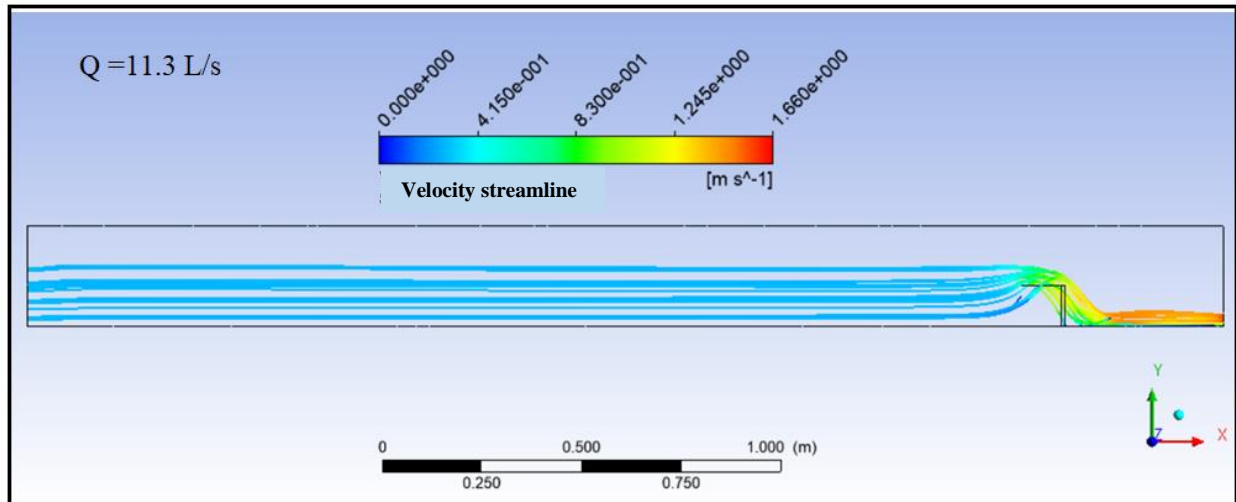


Fig.15. Streamline layout above weir for Q= 10.17 L/sec and P=0.12 m.

The velocity streamlines near bed turned sharply to pass over the weir as the streamline curvatures were very clear. This sharp curvature leads to contacting streamlines with weir wall which created the return flow due to recirculation of streamlines. Whereas,

the streamlines at free surface edge was seen with a reasonably smooth curvature passed over the semi-circular weir. At the downstream section of the weir, the streamlines were far away from the weir wall that makes a space of an air pocket with a hydraulic jump.

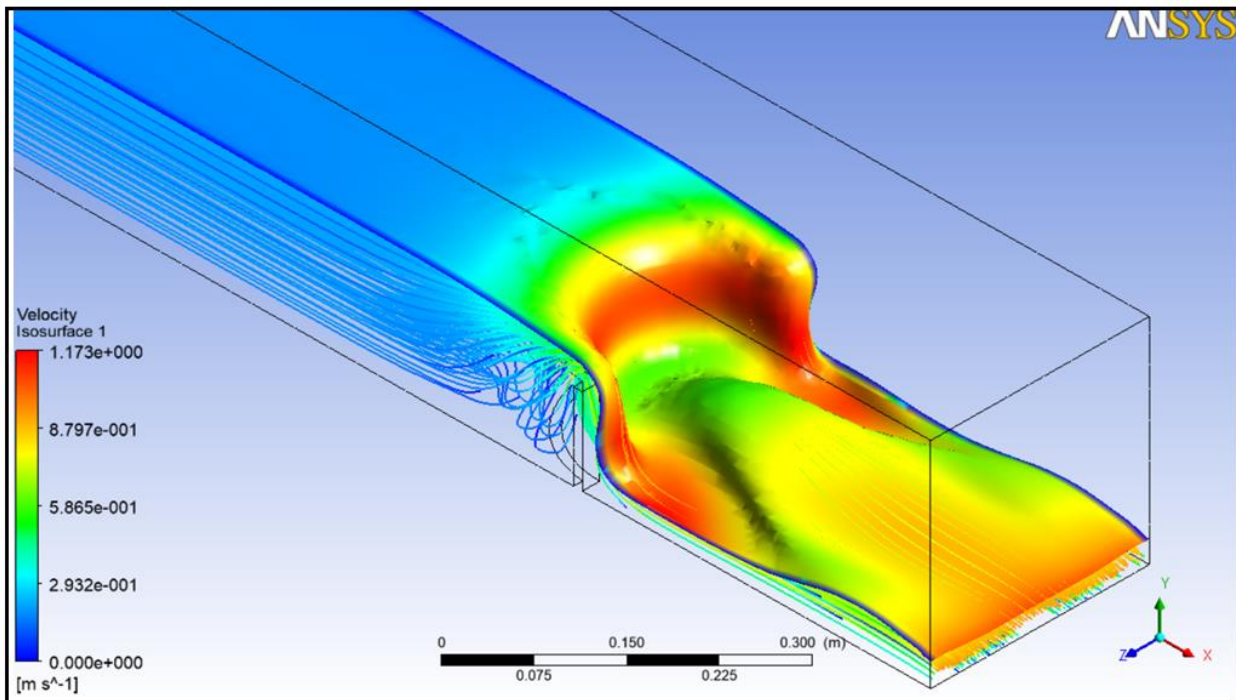


Fig.16. Velocity of isosurface and streamline above weir for Q=5.73 L/sec and P= 0.1m.

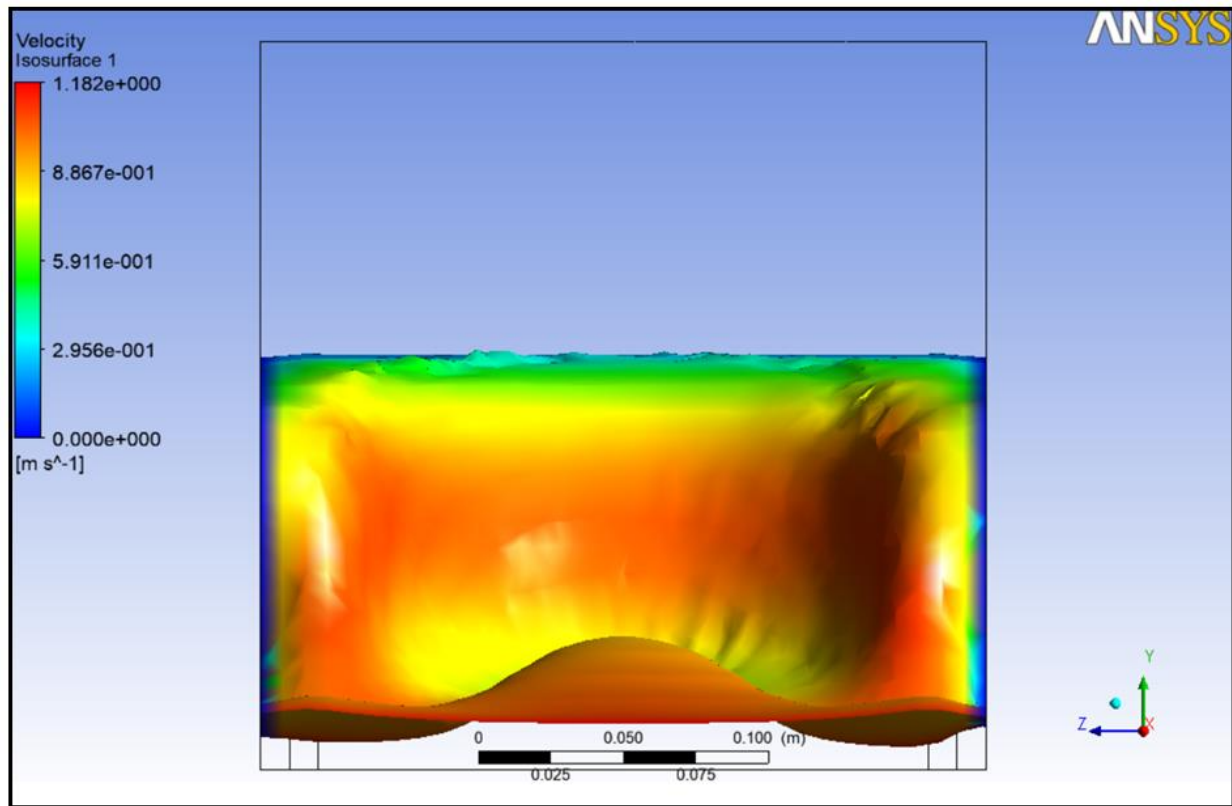


Fig.17. Front view of velocity of isosurface above weir for $Q=5.73\text{L/sec}$ and $P= 0.1\text{m}$.

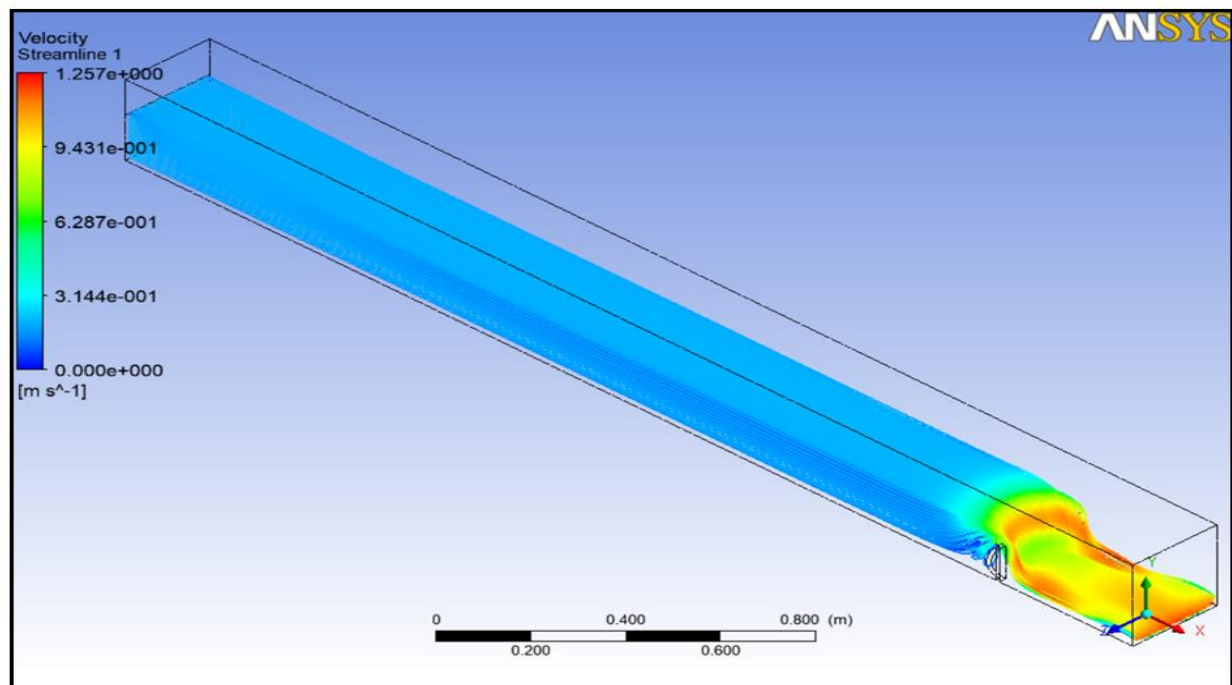


Fig. 18. Face centre of streamlines above weir for $Q= 5.73\text{ L/sec}$ and $P= 0.1\text{m}$.

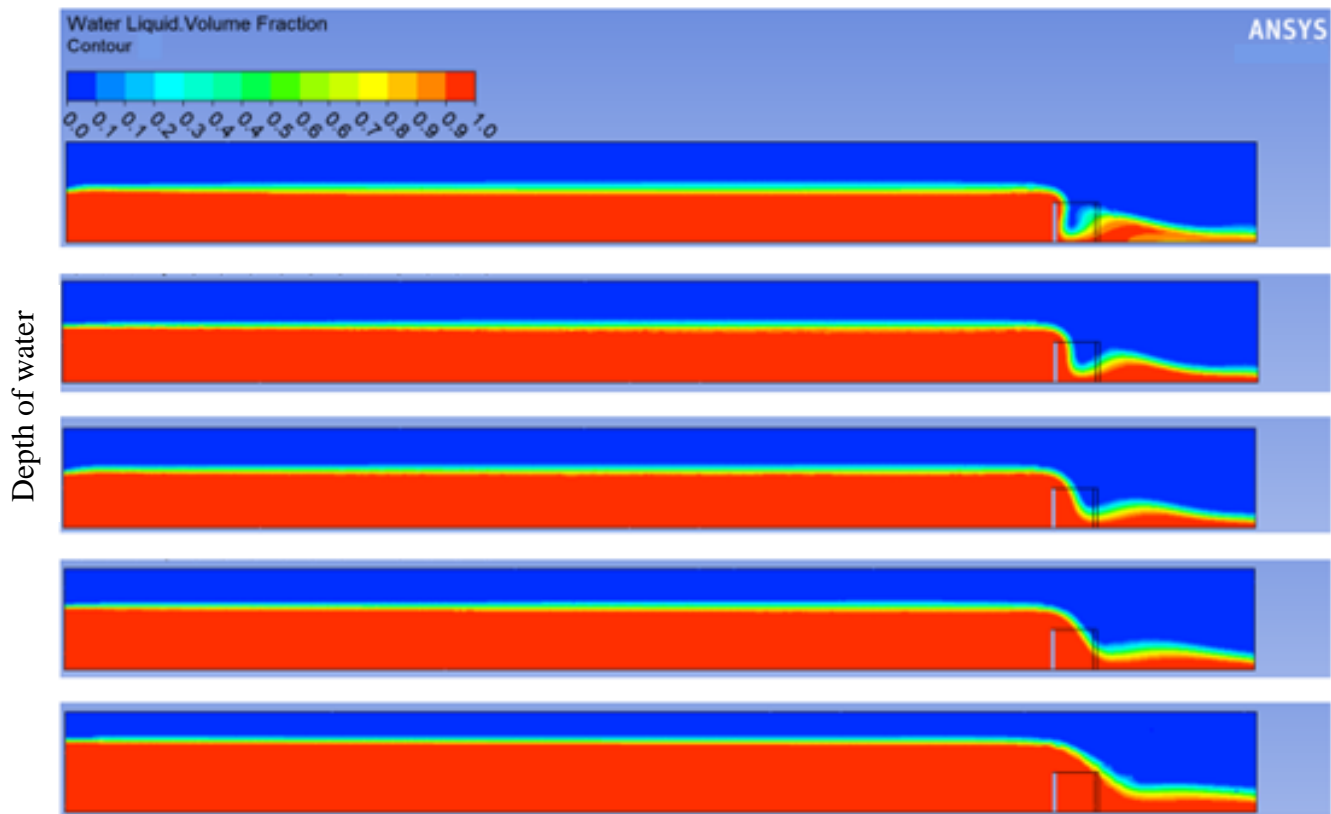


Fig. 19. Free surface profile along the length of the channel for different water depth and velocity

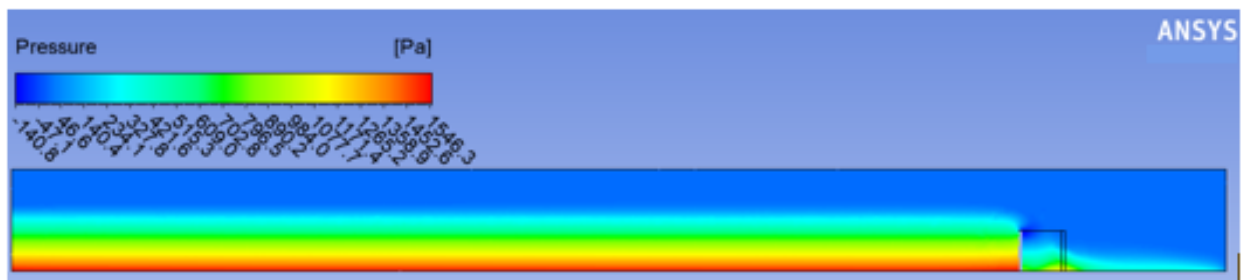


Fig.20. Pressure distribution along the channel for $Q= 4.31$ L/sec

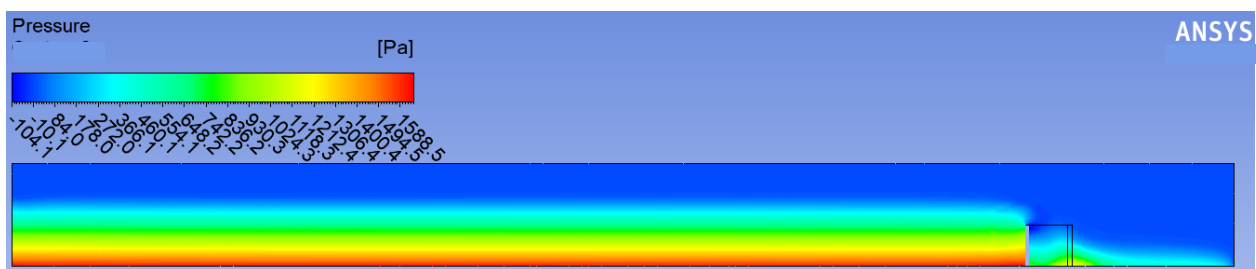


Fig.21. Pressure distribution along the channel for $Q= 5.73$ L/sec

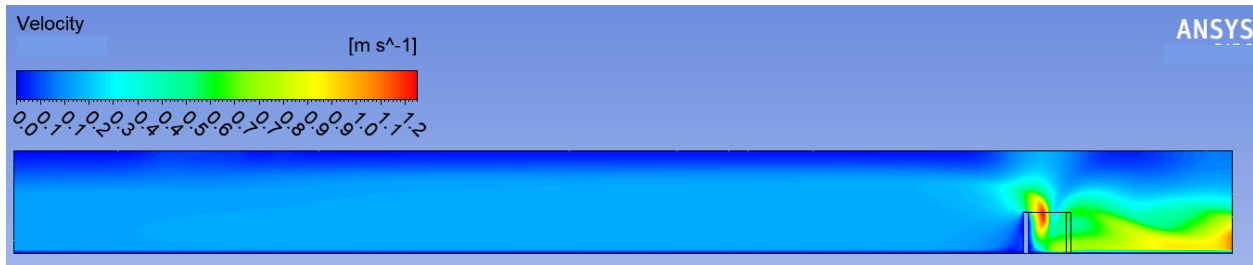


Fig.22. Velocity distribution contours along the channel for $Q= 9.45$ L/sec



Fig .23. Velocity distribution contours along the channel for $Q= 11.3$ L/sec

5. CONCLUSIONS

In the present study, a detailed numerical investigation of water flow past a semi-circular labyrinth weir in a rectangular channel is made. According to the results of this study the conclusions was summarized to the following points:

1. Numerical method was studied the performance of the weir that would be difficult to be calculated experimentally, such as velocity streamlines, pressure distribution and water volume fraction.
2. Qualitative studies of downstream configuration have been made by varying inlet liquid height and water velocity. Homogenous equation with appropriate volume of fraction correlation has been used for simulation.
3. In numerical solutions the free water surface profile was determined by volume of fraction using standard $k-\epsilon$ turbulence model.
4. In numerical investigation, $0.008m$ mesh density is recognized to be a better mesh density, to ensure the flow features spread out through all computational domains with a semi-circular weir.
5. Standard k and epsilon were selected as a specification method for inlet and outlet boundary, finite volume equations were solved through methods of force weighted for pressure and second order scheme for mass, momentum and turbulence model.
6. Mass balance was one of the important criteria for assessing the convergence criteria that showed the differences in mass between inlet and outlet of the channel.

7. The standard k -epsilon model is the best turbulent model for simulating flow over semi-circular weir, because it has the less average percentage of error when its data validated with experimental data.
8. Flow property over semi-circular weir calculated by numerical method, and the residual reached to 1×10^{-1} , with an accurate mass balance between inlet and out let.

REFERENCES

- [1] Carrillo, J. M., Matos, J., & Lopes, R. (2020). Numerical modeling of subcritical flow downstream of a labyrinth weir. 8th IAHR ISHS.
- [2] Crookston, B. M., & Tullis, B. P. (2013). Hydraulic design and analysis of labyrinth weirs. I: Discharge relationships. *Journal of Irrigation and Drainage Engineering*, 139(5), 363-370.
- [3] Desai, R., & Patil, L. (2015). Performance Comparison of Various Labyrinth Side Weirs'. *International Journal of Application or Innovation in Engineering & Management (IJAIEEM)*, 4(6), 68-73.
- [4] Ehsanifar, A., & Ghodsian, M. (2020). Experimental and Numerical Study of Piano Key Weir with Upstream Nose and Semicircular Crest at the Outlet. *Journal of Hydraulics*, 15(2), 31.

- [5] Fluent, A. N. S. Y. S. (2011). ANSYS fluent user's guide, release 14.0. PA: ANSYS Fluent.
- [6] Gabriel, J. D., & John, A. S. (1985). ANSYS Engineering Analysis System User's Manual.
- [7] Jiang, L., Diao, M., Sun, H., & Ren, Y. (2018). Numerical modeling of flow over a rectangular broad-crested weir with a sloped upstream face. *Water*, 10(11), 1663.
- [8] Korkmaz, S., & Ghaznawi, N. A. (2019). Numerical and Experimental Modeling of Flow Over a Broad-Crested Weir. *Sakarya Üniversitesi Fen Bilimleri Enstitüsü Dergisi*, 23(2), 252-258.
- [9] Khalili, M., & Honar, T. (2017). Discharge coefficient of semi-circular labyrinth side weir in subcritical flow. *Water SA*, 43(3), 433-441.
- [10] Mohammed, O.K., 2010. Flow Characteristics through Pipe Culvert Combined with Broad Crested Weir (MSc Thesis, College of Engineering Salahaddin University- Erbil).
- [11] Noori, B. M. A. (2020). Hydraulic performance of circular crested oblique weirs. *Ain Shams Engineering Journal*, 11(4), 875-888.
- [12] Nguyen, C. (2005). Turbulence modeling. *MIT*, 1(8), 1-6.
- [13] Subramanya, K. (2009). *Flow in open channels*. Tata McGraw-Hill Education.
- [14] Safarrazavi Zadeh, M., Esmaeili Varaki, M., & Biabani, R. (2021). Experimental study on flow over sinusoidal and semicircular labyrinth weirs. *ISH Journal of Hydraulic Engineering*, 27(sup1), 304-313.
- [15] Shaghaghian, M., & Sharifi, M. (2015). Numerical modeling of sharp-crested triangular plan form weirs using FLUENT. *Indian Journal of Science and Technology*, 8(34), 1-7.
- [16] Yuce, M. I., Al-Babely, A. A., & Al-Dabbagh, M.A. (2015). Flow simulation over oblique cylindrical weirs. *Canadian Journal of Civil Engineering*, 42(6), 389-407.